Tetrahedron Letters 49 (2008) 6685–6689

Contents lists available at ScienceDirect

Tetrahedron Letters

journal homepage: www.elsevier.com/locate/tetlet

1,2-*O*-(1-Ethylpropylidene)-α-D-glucofuranose, a low molecular mass organogelator: benzene gel formation and their thermal stabilities

Michał Bielejewski [a], Andrzej Łapiński [a], Joanna Kaszyńska [a], Roman Luboradzki [b], Jadwiga Tritt-Goc [a,*]

[a] Institute of Molecular Physics, Polish Academy of Sciences, ul. M. Smoluchowskiego 17, 60-179 Poznań, Poland
[b] Institute of Physical Chemistry, Polish Academy of Sciences, ul. Kasprzaka 44/52, 01-224 Warsaw, Poland

ARTICLE INFO

Article history:
Received 14 July 2008
Revised 1 September 2008
Accepted 10 September 2008
Available online 13 September 2008

Keywords:
Glucofuranose derivative
Benzene gel
Gel–sol transition
Hydrogen-bond network
Solvent dynamic

ABSTRACT

Fourier transform infrared spectroscopy has demonstrated that hydrogen bonds are responsible for the aggregation of 1,2-*O*-(1-ethylpropylidene)-α-D-glucofuranose molecules in solid and benzene gels. The thermal stability of the studied gel is described by its melting temperature T_{GS} and thermal parameters. The deduced value of the gel–sol transition enthalpy is 50 kJ/mol. Viscosity is the major factor which influences the dynamics of the benzene molecules in the gels, as proved by the relaxation measurements.

1. Introduction

The first Letter devoted to the gelation of aqueous solutions by lithium urate appeared in 1841.[1] To date, thousands of other papers on gels have been published but the subject is still very fascinating. The need for more and more materials with various properties for different purposes has accelerated the rapid growth of new gels especially, in the last two decades, molecular gels formed by low molecular-mass organic gelators (LMOG).[2] These can form hydrogels (if the liquid is aqueous), organogels (if the liquid is organic), or both in organic and aqueous media. The gels formed by the LMOGs are physical gels, meaning that only non-covalent interactions such as hydrogen bonding, aromatic (π–π) interactions, van der Waals interactions, ionic or organometallic coordination bonding, or a combination of these are the driving forces responsible for the aggregation of the gelator molecules which in turn leads to the formation of self-assembled fibrillar networks and immobilizes the liquid molecules.[2,3] Most physical gels formed by LMOGs are thermally reversible. The reversible changes between two phases: gel and solution, depend only on the disassembly and assembly of the gelator bonding molecules; their chemical composition remains unchanged in both phases.

Gels formed by low molecular weight organogelators represent an important class of functional materials with potential applications in template materials, biomimetics, as viscosity modifiers in applications such as paints, coatings, oil recovery, in controlled drug release, and in a variety of pharmaceutical and hygienic applications.[2,4,5]

Various aspects of gels made by LMOG and their self-assembled fibrillar networks, describing the theory, techniques used for their study, different types, and their applications, were reviewed in 2006.[2] Despite recent progress toward understanding the molecular basis of gelation and the processes that govern the assembly of gelator molecules into aggregates and even more complicated microstructures,[4] it is still difficult to predict which molecules can serve as gelators. It has been shown that the energies of gel formation are mostly independent of the solvent, but dependent on the gelator structure.[6] The role of the organic solvent in the gel process is poorly understood, but, it is assumed that the solvent molecules are entrapped in the fibrillar networks formed by gelator molecules by capillary forces and are excluded from the gel fibers. However, a study conducted on cholesterol tethered to a *trans*-stilbene and a derivative of mannopyranoside showed that some solvent molecules can be incorporated into the gel fiber.[3,7] LMOGs can be classified according to the criteria based on molecular structure, that is, alkanes, alkanamides, amino acids, peptides, urethanes, and saccharides. Among saccharide-based organogelators, of particular interest are glucofuranose derivatives, which are one of the simplest, smallest, and most efficient gelators.[8] The structure of these compounds is based on a furanose ring with three unprotected OH groups and hydrophobic parts connected to the dioxolane carbon

* Corresponding author. Tel.: +48 061 8695 226; fax: +48 61684524.
E-mail address: jtg@ifmpan.poznan.pl (J. Tritt-Goc).

0040-4039/$ - see front matter © 2008 Elsevier Ltd. All rights reserved.
doi:10.1016/j.tetlet.2008.09.050

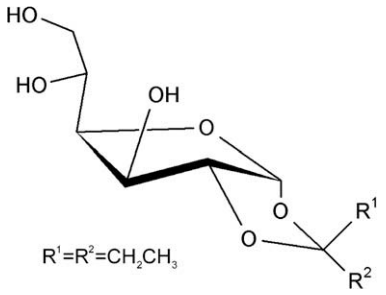

Figure 1. A schematic structure of 1,2-*O*-(1-ethylpropylidene)-α-D-glucofuranose.

atom bridging the dioxolane oxygen atoms (Fig. 1). It has been found that the size and character of the hydrophobic part determines the gelation ability of the saccharide.

A new saccharide-containing gelator, 1,2-*O*-(1-ethylpropylidene)-α-D-glucofuranose (**1**), is the subject of our studies. In recent work, we investigated the molecular dynamics of this compound in the solid state and the thermal properties of its toluene gel.[9,10] Proton spin-lattice relaxation measurements showed that the dipole–dipole interactions between protons of the methyl groups modulated by the C_3 rotation of these groups are the main source of the relaxation.[9] Measurements on 1,2-*O*-(1-ethylpropylidene)-α-D-glucofuranose and its toluene gel demonstrated that the gelator molecules formed a similar hydrogen-bond network in the crystalline and gel state. However, in the gel, one of the stretching bands of the infrared absorption mode of the hydroxyl protons of the gelator is shifted by $\Delta\upsilon_\alpha = 25\ cm^{-1}$ which indicates the involvement of this proton in an interaction with the solvent molecules. Gel–sol phase transition measurements performed as a function of gelator concentration were used to determine the energy of dissolution, 72 kJ/mol.[10] It is also known from literature that the title compound can gelatinize various organic solvents in a wide range of gelator concentration from 0.05% to 4% (g/mL).[8,11–14] Unfortunately, there is no crystal structure and only little information of the microstructure of the xerogel formed by **1** with CCl_4 and toluene exists.[11,12]

In order to learn more about the relationship between the gelator structure in the gel and the crystal structure of the pure gelator, the role of the solvent in gel formation, and the molecular dynamics of solvent molecules in the gel, we undertook studies of the gel derived from **1** and benzene. In this Letter, Fourier Transform Infrared (FT-IR) spectra and the simulated data of the dynamics of the gelator molecule were performed using GAUSSIAN 03, and the thermal properties of the gel and the dynamics of the benzene trapped in the gel are presented and discussed.

2. Molecular conformation

The structure of the title compound is shown in Figure 1; it has three hydroxyl groups, a furanose ring, and a hydrophobic part $R^1 = R^2 = CH_2CH_3$. Due to the hydroxyl groups, the molecules have the ability to form one-dimensional intra-molecular hydrogen-bond networks in the solid state. On the basis of literature,[11,12] data the tendency to form a one-dimensinal intermolecular hydrogen-bond pattern by the gelator molecules in solids is one of the prerequisites for a good gelator.

It can be assumed that the structure of **1** is similar to that of 1,2-*O*-isopropylidene-D-glucofuranose (**2**).[15] The three hydroxyl groups of **2** form a one-dimensional hydrogen bond-network in the crystalline state, and all three OH groups are involved in inter- or intramolecular hydrogen bonds (or in both). The molecules of **2** differ from **1** only in the hydrophobic part, therefore, based on the similarity of the molecular structure we assume a similar arrangement for **1** as in **2**, so the molecular structure of **2** was used as the starting point of the optimization process performed with the use of the program GAUSSIAN 03.

3. FT-IR study of the hydrogen-bond network

The driving forces for aggregation in the case of glucofuranose derivatives are intermolecular interactions that lead to the formation of hydrogen bonds. The Fourier transform infrared (FT-IR) method is very useful in the detection and characterization of hydrogen bonding. The stretching vibrations ν_{OH} along the bond linking atoms or groups of atoms are strongly affected by hydrogen bonding. In monosaccharides, the stretching vibrations ν_{OH} of non H-bonding OH groups occur at about $3600\ cm^{-1}$. Involvement of OH groups in hydrogen bonding leads to shifts of the OH stretching bands to lower wavenumbers.

The relevant parts of the absorption spectra of 1,2-*O*-(1-ethylpropylidene)-α-D-glucofuranose in the crystalline and in the benzene gel-state are shown in Figure 3. The inset shows the FT-IR spectrum of benzene. The IR spectra of the benzene gel and neat solid sample of **1** have no bands at $3600\ cm^{-1}$ as in toluene.[10] So in the benzene gel and in the solid crystalline state, the molecular arrangement allows all the O–H groups to be involved in hydrogen bonding. This association through H-bonding makes the system gelatinize the organic solvent.

Correct assignment of the peaks in the spectra to the O–H stretching modes ν_i of gelator **1**, was possible, thanks to the dynamic simulation of **1** performed with the aid of GAUSSIAN 03.[16] The calculations were carried out on an isolated molecule to determine the response of the molecular dynamics, which dominate in the middle infrared region. The equilibrium geometry and vibrational transitions of the investigated molecule were evaluated at the B3LYP level[17–20] using the basis set 6-311++G(d,p). The starting point for the optimization process was the crystal structure of gelator molecule **2** taken from its X-ray data.[15] The mode description was performed by visual inspection of the individual modes using the GAUSS VIEW program. The proposed assignment was performed based on the experimental and theoretical data, and is presented in Figure 3. The O–H stretching modes ν_α, ν_β, and ν_γ correspond to the O(6)H, O(3)H, and O(5)H hydroxyl protons, respectively, as shown in Figure 2. The calculations on **1** predict the presence of these modes in FT-IR spectra at 3632, 3641, and $3698\ cm^{-1}$, respectively. Such bands are not present in the experimental spectrum, shown in Figure 3, which provides evidence that gelator **1** forms a hydrogen-bond-based network in the crystalline and in the benzene gel-state. However, the FT-IR spectra indicate that the hydrogen-bonding pattern of the gel and the crystal are different, in contrast to the gel made by **1** with toluene, where the hydrogen-bonding network of the gel and crystal were similar to

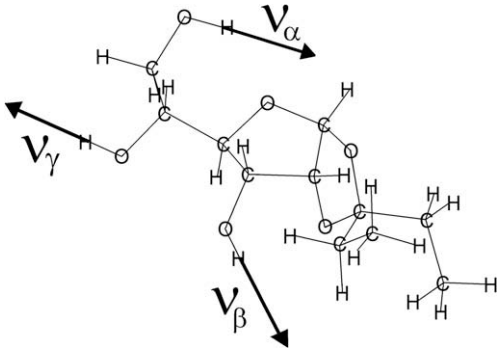

Figure 2. The calculated molecular conformation of 1,2-*O*-(1-ethylpropylidene)-α-D-glucofuranose together with the assigned OH stretching modes ν_i.

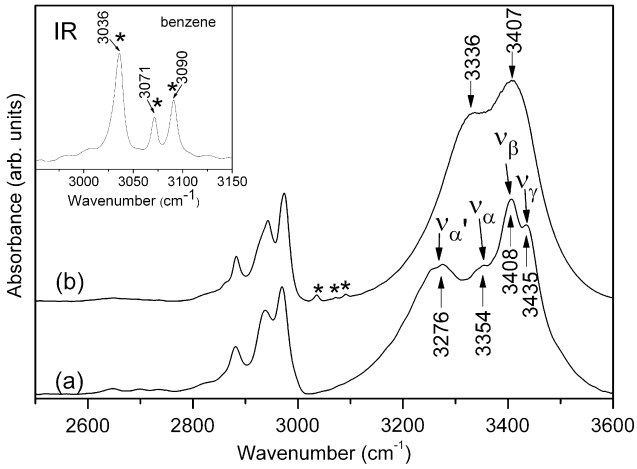

Figure 3. Absorption IR spectra of 1,2-*O*-(1-ethylpropylidene)-α-D-glucofuranose in the crystalline state (a) and in the benzene gel-state (b). The inset shows an IR spectrum of benzene.

each other and only a significant shift of $\Delta\upsilon_\alpha = 25\ cm^{-1}$ was observed upon gelation for absorption modes ν_α.

The FT-IR spectrum of 1,2-*O*-(1-ethylpropylidene)-α-D-glucofuranose in the crystalline state reveals the OH stretching vibrations at 3435 cm^{-1} (ν_γ) and 3408 cm^{-1} (ν_β) and two bands at 3354 cm^{-1} (ν_α) and 3276 cm^{-1} (ν'_α). These modes correspond to the O(5)H, O(3)H, and O(6)H, and O(6)H′ hydroxyl protons, respectively, as shown in Figure 2. Two bands (ν_α) and (ν'_α) were assigned to the O(6)H hydroxyl protons of two crystallographically different molecules as shown by the X-ray data of compound **2**.[15] The molecules differ slightly in the angles and lengths of the bonds in the O(6)H vicinity. The different arrangement of the O(6)H protons influences the strength of the hydrogen bonds formed by them which is reflected in the FT-IR spectra.

In the benzene gel of **1**, only two peaks are present at 3336 cm^{-1} and 3407 cm^{-1}, respectively. The IR spectra of **1** in the solid and gel state have OH stretching vibrations between 3200 cm^{-1} and 3500 cm^{-1} consistent with the involvement of the OH protons in hydrogen-bond networks. However, comparison of these spectra clearly demonstrate the differences in the self-assembly of the molecules in both states. Upon gelation, two peaks (ν_α) and (ν'_α) merged into one single peak at 3336 cm^{-1}. This suggests that in the gel, the gelator molecules become crystallographically equivalent and form hydrogen bonds of equal strength, intermediate compared with the solid state. The other two peaks (ν_γ) and (ν_β) strongly overlap in the gel spectrum and gave one band at 3407 cm^{-1} related to the OH stretching vibrations. Therefore, we can conclude that the hydrogen-bond network formed by the gelator molecules of **1** in the gel state is more 'homogeneous' as to the strength of its hydrogen bonds compared to the network in the solid state or to the same network in the toluene gel.[10] The different hydrogen-bonding pattern of the benzene and toluene gel of the same gelator **1** indicates the influence of the solvent on the gel formation. The shift of OH stretching bands (ν'_α) upon gelation of **1** in benzene occurs at higher wavenumbers as compared with this shift in toluene gel. This indicates a lower strength of the intermolecular hydrogen bond interaction formed by O(6)H hydroxyl in **1** with benzene than in toluene and should lead to the formation of gelator aggregates of shorter lengths. This fact in turn should be reflected in a different microstructure of the network in both gels.

The FT-IR spectra for a 3% (g/mL) benzene gel and for a 1% (g/mL) were the same. The similarity of the experimental FT-IR spectra and theoretical data suggests that the molecular conformation of gelator **1** is indeed as presented in Figure 2.

4. The gel–sol phase transition

Figure 4 shows the gel–sol transition temperatures (T_{GS}) of the benzene gel based on 1,2-*O*-(1-ethylpropylidene)-α-D-glucofuranose as a function of the gelator concentration. The T_{GS} temperature is defined by the temperature at which a gel in a sealed tube starts to flow when heated in a continuous nitrogen gas flow. The whole phase transition (the dissolution of all the gel) occurs over a temperature range of about 15 K for all the studied gel concentrations. The observed broad range of the phase transition indicates the nonhomogeneous microstructure (i.e., built from different aggregates of gelator molecules) of the hydrogen-bond networks within the studied gel like as in the toluene based gel.[10]

From Figure 4, we can see that the T_{GS} values increased to 347 K with an increase of concentration up to 2% (g/mL). Above 2% (g/mL), no dependence of the phase transition on concentration was observed. Remarkably, the T_{GS} value for benzene-based gel **1** at 4% (g/mL) is 350.9 K and is very close to the boiling point of benzene (353.2 K), which reflects the high stability of the self assemblies of gelator molecules in benzene. A concentration-independent (plateau) region was not observed for the toluene gel in the same range of concentration.[10] As the T_{GS} for the benzene and toluene gels were determined using the same method, we can conclude that different thermal stabilities observed for both gels formed by **1** can be attributed only to the solvent properties.

It is accepted that the gel-to-sol phase transition can be considered as a dissolution process of microcrystals, and is described by Eq. 1 derived from Schrader's relation[6]

$$\log[C] = -\frac{\Delta H}{2.303R} \times \frac{1}{T_{GS}} + \text{constant} \quad (1)$$

where C is the gelator concentration, ΔH is the melting enthalpy, R is the gas constant, and T_{GS} is the gel-to-sol transition temperature.

This expression was originally proposed for the gel-to-sol phase transition for polymeric networks whose crosslink formation is made up of pairs of chains. Eq. 1 does not take into account the influence of the solvent, which may affect the structures and thermodynamic behaviors.[21] Therefore, using Eq. 1 for describing the physical gel is probably oversimplified but is generally accepted.

In Figure 5, the logarithm of the concentration of **1** is plotted versus the reciprocal transition temperature. The gel–sol transition enthalpy ΔH was determined to be 50 kJ/mol. This value corresponds well with the values reported up to now for the other monosaccharides-based gels[22] but is much lower than for the toluene gel made by **1**.[10] As the ΔH values are relative to the strength of the intermolecular interactions (mainly hydrogen bonding) in

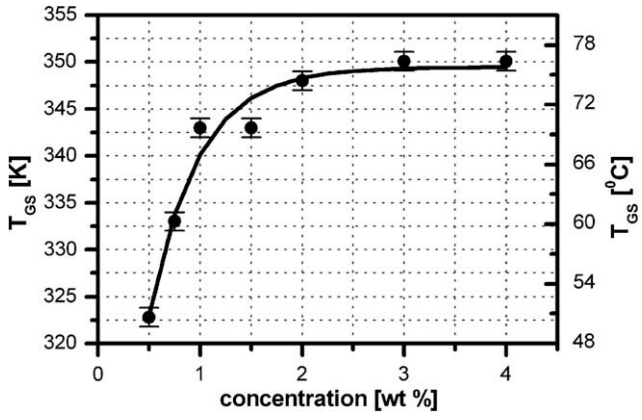

Figure 4. Dependence of T_{GS} on the concentration of 1,2-*O*-(1-ethylpropylidene)-α-D-glucofuranose gel in benzene. The solid line has no physical meaning and is included as a visual guide.

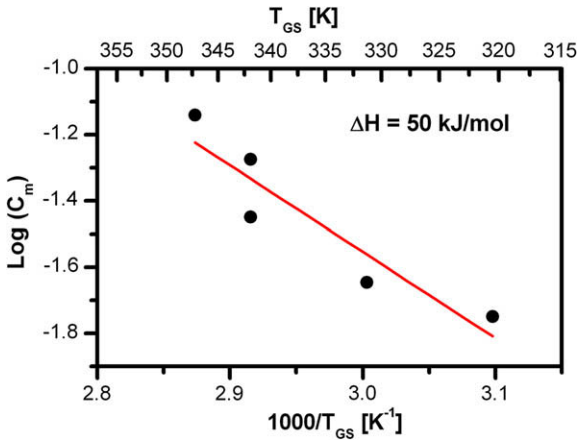

Figure 5. Plot of the logarithm of gelator concentration versus the reciprocal absolute temperature of T_{GS}. The solid line is the best fit of Eq. 1 to the experimental points.

the nanofiber, the lower ΔH value in benzene gel **1** than in the toluene gel is caused by the lower intermolecular interactions. This result is consistent with our FT-IR measurements which showed that at least O–H stretching bands (ν'_{α}) upon gelation of **1** in benzene are shifted to higher wavenumbers when compared with this shift in toluene gel.

5. The dynamics of benzene in the gel network

The molecular mobility of the benzene molecules in the gel state, solution, and in bulk benzene were studied through proton spin-lattice relaxation measurements. The motions of gelator molecule aggregates are strongly restricted in the gel and are undetectable under our NMR measuring conditions (no high resolution measuring conditions). Therefore, we measured only the relaxation of the benzene protons. Table 1 presents the proton spin-lattice relaxation data measured in 1% (g/mL) and 3% (g/mL) gels at room temperature and at 358 K, the temperature at which both gels are in a solution state. For comparison, the values of T_1 for bulk benzene are also given in Table 1. As can be seen, the measured spin-lattice relaxation times of benzene in the gels at 298 K are shorter than in benzene itself. This finding can be attributed to the increased viscosity and reduced mobility of the solvent which is entrapped within the hydrogen-bond network formed by the gelator; and the possible interaction between the benzene molecules and gelator aggregates which facilitate a rapid dissipation of spin energy to the gel matrix. If the last factor contributes to the observed decrease of the relaxation time of benzene in the gel, then we have to assume the exchange model of the bulk benzene (the molecules in the large pores within the gel network of the hydrogen-bond gelator aggregates) and benzene molecules interacting with the gelator molecules which form the pore surfaces. If so, non-exponential recovery of the magnetization would be expected because the surface-dominated relaxation is reflected in the distribution of the relaxation times. This is not the case observed in our relaxation measurements.

Table 1
T_1 values of the solvent protons measured at 300 MHz for 1,2-*O*-(1-ethylpropylidene)-α-D-glucofuranose benzene gel and for bulk benzene

	1% (g/ml) gel	**3**% (g/ml) gel	Benzene
T_1 (gel) 298 K	9.3 s	8.7 s	10.3 s
T_1 (melt) 358 K	20.8 s	19.6 s	21.5 s

We can also rule out significant influences of the confinement effect on the relaxation in benzene gel **1**. It is known that 1,2-*O*-(1-ethylpropylidene)-α-D-glucofuranose, like other low molecular weight gelators in organic solvents, self-assembles into, for example, elongated fiber-like structures through hydrogen interaction. These fibers in turn, at T_{SG} (sol–gel), form a three dimensional network encapsulating the solvent molecules. Thus, it is reasonable to assume that the benzene molecules are entrapped in the spaces (often called pores) between the entangled fibrils, which can limit their molecular freedom and consequently reduces their mobility. However, above the phase transition T_{GS}, the gelator aggregates disassemble and the macroscopic flow of the sample is free. Thus, the same relaxation times should be observed for benzene in solution (upon gel melting) as for bulk benzene if the confinement effect is the only factor which influences the relaxation of the benzene in the gel. A short inspection of the T_1 values at 358 K given in Table 1 showed that upon gel melting, the measured relaxation time is still lower than for bulk benzene. This fact indicates that as in a variety of cholesterol derivative gelators and also in the benzene gel made from 1,2-*O*-(1-ethylpropylidene)-α-D-glucofuranose, the pores in the gels are sufficiently large and do not significantly restrict the motion of solvent.

Therefore, in the studied gel we can assume that the observed decrease of benzene T_1 in the gels when compared to bulk benzene is mainly due to the viscosity effect. Then, the T_1 is intramolecular in origin,[23] and in the fast motion limit it is proportional to the correlation time ($\frac{1}{T_1} \propto \tau_c$). The correlation time can be expressed as

$$\tau_c = \frac{4\pi\eta a^3}{3k_B T} \quad (2)$$

where η is the viscosity and a the radius of the molecule. The larger viscosity of benzene in the gel indicates a smaller value for the relaxation time when compared to bulk benzene. The differences between the values of T_1 observed for the gels at the same temperatures are attributed to the different gelator concentrations: 1% (g/mL) and 3% (g/mL).

6. Optical polarization microscopy observation of aerogel

To obtain visual insight on the microstructure of the gelator network, the gel sample of **1** was investigated by optical polarization microscopy. The optical microscopy image is presented in Figure 6. It is evident from these micrographs that gelator **1** forms

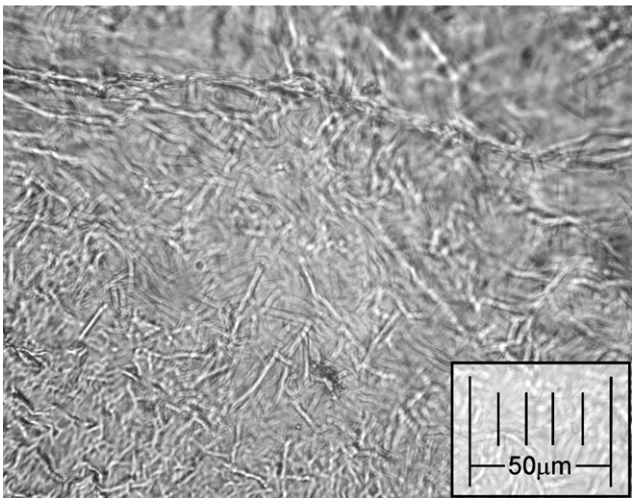

Figure 6. Optical polarization microscopy image of benzene gel at a 3% (g/mL) concentration of gelator **1**.

in benzene a network consisting of fibers with an approximate diameter of about 2 μm.

In conclusion the FT-IR measurements performed on 1,2-*O*-(1-ethylpropylidene)-α-D-glucofuranose in the solid and benzene gels showed that the molecules formed a hydrogen-bonding network in both states. However, some influence of the solvent is noticeable in the gel spectra as they differ from that in the solid state.

The determined value of the gel–sol transition enthalpy (50 kJ/mol) corresponds well with the values reported for the other monosaccharides-based gels[22] but is much lower than for the toluene gel made by **1**.[10] We conclude that the lower ΔH value is attributed to the lower intermolecular hydrogen-bonding interactions in the benzene gel. This conclusion is proved by our FT-IR measurements which showed that the O–H stretching bands (ν'_α), upon gelation of **1** in benzene are shifted to higher wavenumbers as compared with this shift in toluene gel. The most important factor which influences the dynamics of the benzene molecules in the gels made by **1** is the viscosity as proved by the relaxation measurements.

7. Preparation of 1,2-*O*-(1-ethylpropylidene)-α-D-glucofuranose (1) and its benzene gel

The LOMG (**1**) was synthesized by the method described.[7,11] Concentrations of 0.5%, 1%, 2%, 3%, and 4% (g/mL) of **1** were chosen to form the gels studied in the present work. In order to prepare a gel, the appropriate amount of the gelator was mixed with benzene in a closed capped tube; the mixture was heated until the solid dissolved (the solvent boiling point was reached during this process) and then kept at this temperature for a few seconds to obtain a homogeneous liquid. Next, the solution was cooled to room temperature and left for a few minutes. As a result, a clear, transparent gel was obtained for each concentration.

8. Apparatus for spectral and proton relaxation measurements

The absorption IR spectra of benzene, powdered crystals of **1** and its benzene gel dispersed in KBr pellets were measured in the frequency range from 400 cm^{-1} to 7000 cm^{-1}, at room temperature. The spectral resolution of FT-IR spectra was 2 cm^{-1}.

The ^1H NMR spin-lattice relaxation measurements were carried out on a Bruker AVANCE pulse spectrometer operating at 300 MHz using a 180^o–τ–90^o pulse sequence in the temperature range of (298–360) K. The temperature of the sample was controlled by means of a continuous nitrogen gas-flow system and determined to an accuracy of ±0.1 K. The recovery of the magnetization was found to be exponential within an experimental error at all temperatures. The errors in the measurements of T_1 were estimated to be about 3%.

9. Gel–sol phase transition measurements

Transition temperatures were determined using the air-bath method and visual inspection of the samples. The air-bath method involves inserting a sample into a stream of continuous nitrogen gas flow whose temperature changes are precisely controlled. For this purpose, we used a slightly modified NMR probe head. The opaque RF coil was replaced by a transparent glass tube and thus a visual inspection of the sample was possible. The temperature of the gel–sol (T_{GS}) transition was determined upon heating the sample to the temperature at which the system starts to flow and was measured with an accuracy of ±0.1 °C.

10. Optical polarization microscopy measurements

For imaging, a 3% (g/mL) gel sample was carefully placed, using a pipette, at the center of a glass microscope slide. A JENAPOL microscope operating in differential interference contrast and polarization modes was used.

Acknowledgment

This work has been supported by funds for sciences in years 2007–2009 as research project N N202 1441 33

References and notes

1. Von Lipowitz, A.; Liebigs, P. *Ann. Chem. Pharm.* **1841**, *38*, 348–355.
2. Weiss, R. G.; Terech, P. *Molecular Gels, Materials with Self –Assembled Fibrillar Network*, Springer: Dordrecht, The Netherlands, **2006**.
3. Geiger, C.; Stanescu, M.; Chen, L.; Whitten, D. G. *Langmuir* **1999**, *15*, 2241–2245.
4. Terech, P.; Weiss, R. G. *Chem. Rev.* **1997**, *97*, 3133–3159.
5. Gronwald, O.; Snip, E.; Shinkai, S. *Curr. Opin. Colloid Interface Sci.* **2002**, *7*, 148–156.
6. Murata, K.; Aoki, K.; Suzuki, T.; Hanada, T.; Kawabata, H.; Komori, T.; Oseto, F.; Ueda, K.; Shinkai, S. *J. Am. Chem. Soc.* **1994**, *116*, 6664–6674. and references cited therein.
7. Sakurai, G.; Jeong, Y.; Koumoto, K.; Friggeri, A.; Gronwald, O.; Sakurai, S.; Okamoto, S.; Inoue, K.; Shinkai, S. *Langmuir* **2003**, *19*, 8211–8217.
8. Luboradzki, R.; Gronwald, O.; Ikeda, M.; Shinkai, S.; Reinhoudt, D. N. *Tetrahedron* **2000**, *56*, 9595–9599.
9. Bielejewski, M.; Rachocki, A.; Luboradzki, R.; Tritt-Goc, J. *Appl. Magn. Reson.* **2008**, *33*, 431–438.
10. Tritt-Goc, J.; Bielejewski, M.; Luboradzki, R.; Łapiński, A. *Langmuir* **2008**, *24*, 534–540.
11. Luboradzki, R.; Pakulski, Z. *Tetrahedron* **2004**, *60*, 4613–4616.
12. Luboradzki, R.; Pakulski, Z.; Sartowska, B. *Tetrahedron* **2005**, *61*, 10122–10128.
13. Grigoriew, H.; Luboradzki, R.; Gronkowski, G. *J. Non-Cryst. Solids* **2006**, *352*, 3052–3057.
14. Grigoriew, H.; Gronkowski, G. *J. Non-Cryst. Solids* **2006**, *352*, 5492–5497.
15. Takagi, S.; Jeffrey, A. *Acta Crystallogr. B* **1979**, *35*, 1225–1522.
16. Frisch, M. J.; Trucks, G. W.; Schlegel, H. B.; Scuseria, G. E.; Robb, M. A.; Cheeseman, J. R.; Montgomery, J. A. Jr.; Vreven, T.; Kudin, K. N.; Burant, J. C.; Millam, J. M.; Iyengar, S. S.; Tomasi, J.; Barone, V.; Mennucci, B.; Cossi, M.; Scalmani, G.; Rega, G.; Petersson, G. A.; Nakatsuji, H. Hada, M.; Ehara, M.; Toyota, K.; Fukuda, R.; Hasegawa, J.; Ishida, M.; Nakajima, T.; Honda, Y.; Kitao, O.; Nakai, H.; Klene, M.; Li, X.; Knox, J. E.; Hratchian, H. P.; Cross, J. B.; Adamo, C.; Jaramillo, J.; Gomperts, R.; Stratmann, R. E.; Yazyev, O.; Austin, A. J.; Cammi, R.; Pomelli, C.; Ochterski, J. W.; Ayala, P. Y.; Morokuma, K.; Voth, G. A.; Salvador, P.; Dannenberg, J. J.; Zakrzewski, V. G.; Dapprich, S.; Daniels, A. D.; Strain, M. C.; Farkas, O.; Malick, D. K.; Rabuck, A. D.; Raghavachari, K.; Foresman, J. B.; Ortiz, J. V.; Cui, Q.; Baboul, A. G.; Clifford, S.; Cioslowski, J.; Stefanov, B. B.; Liu, G.; Liashenko, A.; Piskorz, P.; Komaromi, I.; Martin, R. L.; Fox, D. J.; Keith, T.; Al-Peng, C. Y.; Nanayakkara, A.; Challacombe, M.; Gill, P. M. W.; Johnson, B.; Chen, W.; Wong, M. W.; Gonzalez, C.; Pople, J. A. GAUSSIAN 03, Revision B.05, Gaussian, Inc., Pittsburgh, PA, **2003**.
17. Becke, A. D. *Phys. Rev. A* **1988**, *38*, 3098–3100.
18. Becke, A. D. *J. Chem. Phys.* **1993**, *98*, 5648–5652.
19. Lee, C.; Yang, W.; Parr, R. G. *Phys. Rev. B* **1988**, *37*, 785–789.
20. Scott, A. P.; Radom, L. *J. Phys. Chem.* **1996**, *100*, 16502–16513.
21. Garner, C. M.; Terech, P.; Allegraud, J. J.; Mistrot, B.; Nguyen, P.; de Geyer, A.; Rivera, D. J. *Chem. Soc., Faraday Trans.* **1998**, *94*, 2173–2179.
22. Gronwald, O.; Sakurai, K.; Luboradzki, R.; Kiura, T.; Shinkai, S. *Carbohydr. Res.* **2001**, *331*, 307–318.
23. Levitt, M. H. *Spin Dynamics. Basics of Nuclear Magnetic Resonance*, John Wiley & Sons: Chichester, England, **2003**.